Using the lambda function to evaluate probe measurements of charged dielectric surfaces

Rerup, T. O.; Crichton, George C; McAllister, Iain Wilson

Published in:
IEEE Transactions on Dielectrics and Electrical Insulation

Link to article, DOI:
10.1109/94.556558

Publication date:
1996

Document Version
Publisher's PDF, also known as Version of record

Using the λ Function to Evaluate Probe Measurements of Charged Dielectric Surfaces

T. O. Rerup, G. C. Crichton and I. W. McAllister

Department of Electric Power Engineering, Technical University of Denmark, Lyngby, Denmark

ABSTRACT

The use of Pedersen's λ function to evaluate electrostatic probe measurements of charged dielectric surfaces is demonstrated. With a knowledge of the probe λ function, the procedure by which this function is employed is developed, and thereafter applied to a set of experimental measurements available in the literature. The values of surface charge density derived are in good agreement with the published data. Through this field-theoretical approach, it is readily shown that areas of charge remote from the probe location can produce a major part of the probe signal. If a circuit-theory approach were adopted to analyze such probe measurements, then as the field features of the probe response cannot be taken into account, a serious misinterpretation of the measurements could arise.

1. INTRODUCTION

With the development of HVDC-GIS, a need has arisen for the study of surface charge on insulating materials. During the last 30 years, electrostatic probes were developed and used for the measurement of charge on dielectric surfaces. In general, these studies based their analysis on the circuit-theory approach developed in the sixties by Davies [1]. However, in the mid-eighties it was realized that a correct interpretation of measured probe data required a proper field solution which considered the entire dielectric surface and system boundaries [2–5]. To facilitate the analysis of such measured data, Pedersen introduced a probe response function, the λ function [3].

In the present paper, this function is used to illustrate the manner in which a distribution of surface charge density and the associated probe response are mathematically coupled together. The procedure is first developed and thereafter applied to the independent measurements of Yashima *et al.* [4]. From their study of a charged dielectric surface, the following data are available

1. the directly measured values of surface charge (Faraday cage technique)
2. the measured probe response (induced charge)
3. the calculated surface charge densities (via the probe response).

Using the λ function and the measured probe response 2, it is possible to determine a unique surface charge distribution, which is then compared with 1 and 3 above. Despite a software limitation on our λ evaluation (2D *vs.* 3D calculation), the agreement is good. In addition, from a detailed examination of the intermediate steps in the analysis, each probe response could mathematically be resolved into the contributions from individual surface areas. Thus the effect on the total probe signal from areas of charge remote from the probe location could be quantitatively assessed.

2. THE λ FUNCTION

Pedersen's λ function relates the Poissonian induced charge dq [6] on the sensor plate of the probe to the dielectric surface-charge dQ; *viz.*

$$dq = -\lambda dQ \tag{1}$$

This relationship assumes that the permittivity of the dielectric is independent of field strength. If the volume charge density within the solid dielectric is assumed to be *zero*, then with respect to the contributions from all surface elements of charge we have

$$q = -\iint_{A_0} \lambda\sigma \, dA \tag{2}$$

in which q is the total Poissonian induced charge on the sensor plate, and σ is the surface charge density on the surface element dA of A_0, the surface of the solid dielectric. If a charge exists within the bulk of the dielectric, (2) would contain an additional term [3, 7].

The dimensionless parameter λ is a solution of the general Laplace equation for the complete system geometry [3, 7], *i.e.*

$$\vec{\nabla} \cdot (\varepsilon \vec{\nabla} \lambda) = 0 \tag{3}$$

1070–9878/96/ $3.00

The boundary conditions are $\lambda = 1$ at the sensor plate of the probe and $\lambda = 0$ at all other electrodes. In addition, at dielectric interfaces the normal derivatives of λ must obey the condition

$$\varepsilon_+ \left(\frac{\partial \lambda}{\partial n}\right)_+ = \varepsilon_- \left(\frac{\partial \lambda}{\partial n}\right)_- \tag{4}$$

where the + and − signs refer to the opposite sides of the interface: see [3, 7]. Because (3) is simply Laplace's equation, Ansoft Corporation's Maxwell EM Field Simulator (2D version) was used to evaluate the variation of λ at the dielectric surface.

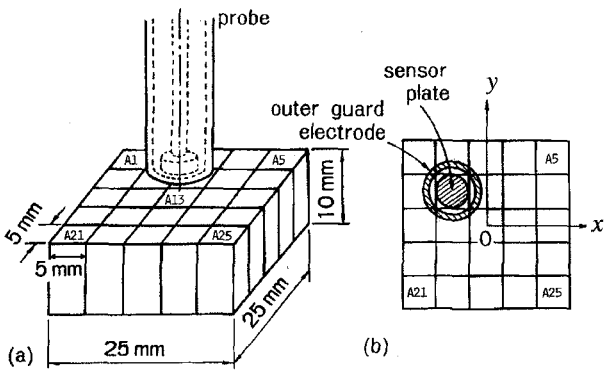

Figure 1. System geometry [4].

3. SYSTEM GEOMETRY

The geometry of [4] is shown in Figure 1. In [4] the charged dielectric surface was made of 25 removable solid polytetrafluoroethylene blocks each of upper surface area 5×5 mm^2 and with a height of 10 mm. The total specimen has a square surface of area of 25×25 mm^2. The probe consists of a sensor plate of radius of 2.5 mm, with a guard ring of inner radius of 3.5 mm and outer of 4.5 mm radius. The height of the probe sensor plate above the dielectric surface is held constant at 1 mm. The length of the probe body is not stated in [4], but in the present study we set this to 95 mm. As this dimension is $\gg$ 1 mm, it becomes of minor importance in the evaluation of the λ function. The 2D λ calculation mentioned in the Introduction will be discussed in Section 4.

We number the 25 blocks consecutively; *i.e.* from A1 to A25, see Figure 1, with the corresponding surface areas designated A_1 to A_{25}. This procedure simplifies the mathematical development in the ensuing analysis. It can be seen in Figure 1 that the center of block A1 has the coordinates $x = -10$ mm, $y = 10$ mm, and that the center of block A13 has the coordinates $x = 0$, $y = 0$.

The data available from the study of Yashima *et al.* [4] are their surface charges measured directly by means of a Faraday cage apparatus and converted into surface charge densities; their measured probe responses (total Poissonian induced charge on the sensor plate), and thereafter their derived surface charge densities. With reference to Figure 8 of [4], the pertinent numerical data were made available directly by these authors, and are as follows.

The magnitude of surface charge density σ_F (μC/m^2) from the Faraday cage study is

$$\sigma_F = \begin{pmatrix} 15.0 & 12.9 & 13.4 & 0.96 & 12.6 \\ 13.3 & 11.6 & 12.2 & 1.5 & 13.0 \\ 14.3 & 12.2 & 12.6 & 1.4 & 12.0 \\ 6.6 & 11.4 & 14.0 & 1.4 & 12.0 \\ 5.0 & 12.4 & 13.6 & 2.3 & 14.0 \end{pmatrix} \tag{5}$$

The measured probe response p (pC) is

$$p = \begin{pmatrix} 252 & 295 & 271 & 136 & 194 \\ 297 & 347 & 312 & 175 & 244 \\ 310 & 358 & 329 & 180 & 248 \\ 235 & 319 & 314 & 163 & 235 \\ 144 & 261 & 262 & 140 & 204 \end{pmatrix} \tag{6}$$

The magnitude of the surface charge density σ_D (μC/m^2) derived on the basis of the total system geometry and probe response is

$$\sigma_D = \begin{pmatrix} 11.5 & 12.6 & 11.9 & 1.8 & 9.6 \\ 12.2 & 13.5 & 12.0 & 2.8 & 11.6 \\ 13.3 & 13.9 & 12.8 & 2.5 & 11.3 \\ 8.6 & 12.2 & 12.7 & 1.8 & 10.9 \\ 3.8 & 11.5 & 11.7 & 2.3 & 10.5 \end{pmatrix} \tag{7}$$

It should be noted that to enhance clarity in (5), (6) and (7), a 5×5 array has been used whenever values corresponding directly with the 25 blocks are considered. The first row represents A1 to A5, the second row A6 to A10 and so forth. According to Figure 8 of [4], the surface charges are negative. However it is uncertain whether the stated probe response is the Poissonian induced charge or the Laplacian induced charge, see [6]. Normally, the Laplacian induced charge is measured via the probe either as the voltage over a known capacitor, or as the charge flow in the lead connecting the probe sensor plate to ground. However as these induced charge components are numerically equal, and as the surface charges in [4] are unipolar, we will simply perform our calculations using numerical values. Such a simplification should of course not be undertaken in practice, because surface charges of *both* polarities could be present.

4. SIMULATION

As mentioned previously, a 2D finite-element software package is used to determine the λ function. As the charged dielectric surface used in [4] is square in form (25×25 mm^2), a correct calculation of the λ function would require a 3D program. We did not possess this capability, and it was necessary to adapt our system to the available 2D software. Hence, we represent their system geometry by a large disc of polytetrafluoroethylene (relative permittivity $\varepsilon_r = 2.0$) of thickness 10 mm and radius 100 mm. As in [4], the probe was placed 1 mm above the dielectric surface of the disc. It should be noted that the radius of the disc is made substantially larger than the diagonal ($25\sqrt{2}$ mm) of the original square dielectric system in [4].

With the probe located on the disc axis, the variation of λ across the upper dielectric surface is shown in Figure 2. Due to the axially symmetric nature of our model geometry, the calculated λ function is also axially symmetric with respect to the axis of the probe. Hence

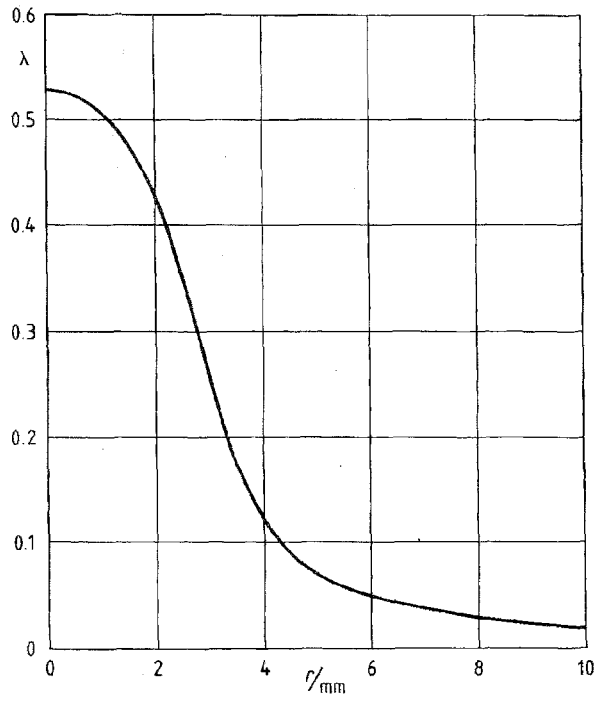

Figure 2. Variation of the λ function across the surface of the dielectric. $r = \sqrt{x^2 + y^2}$ represents the radial distance from the probe axis.

the value of the λ function at any given point on the dielectric surface is determined exclusively by the normal distance from the probe axis to the point in question. The λ calculation is undertaken for the PTFE disc, the radius of which is approximately 3× the diagonal of the square geometry in [4]. Hence in our analysis the same λ function can be employed within the central area of the disc, irrespective of the position of the probe, as the error introduced is negligible. This approximation for the true λ function is discussed in Section 7.I.I.

5. THE Λ MATRIX AND EVALUATION OF SURFACE CHARGE DENSITY

To evaluate the charge distribution on the dielectric surface requires a multipoint measurement to be performed with the probe. Such a technique generates a series of probe responses. Each response is related to the specific position (x, y) of the probe relative to the selected origin on the dielectric surface. In the present case, owing to the symmetry and identical nature of the blocks, the probe positions are taken in turn above the center point of each of the 25 blocks. Yashima *et al.* [4] adopted the same probe locations in their evaluation.

If the charge per block is assumed to be uniformly distributed over the upper surface of the block, then a uniform surface density σ_j may be assigned to each block. Consequently, the magnitude of the charge induced on the probe by a single block may be expressed as

$$|q| = \sigma_j \iint \lambda \, dA \tag{8}$$

Because the integral in (8) contains only λ and surface area, we are able to take into account simultaneously both the geometrical scanning procedure and the λ function by introducing a Λ matrix. The formation of this matrix must correspond with the 25 blocks. For each probe position (block center), a sub-matrix is derived with 1×25 elements, with each element given by

$$\Lambda_{ij} = \iint_{A_j} \lambda_i \, dA \tag{9}$$

where dA is a surface element of A_j. The index i refers to the position of the probe while j relates to the surface area in question. The subscript i in λ_i indicates that, in general, the λ values associated with a block are dependent upon the position of the probe. Each sub-matrix element is directly connected with the discretization of the charged surface area, and as the λ function itself is dimensionless, the dimension of the Λ matrix is that of area.

With the probe fixed in a position directly above the area element A_i, the contribution to the probe response (induced charge) from surface charge element σ_j of surface area A_j is given by $\Lambda_{ij}\sigma_j$. By summation of all the contributions for $j = 1$ to 25, the total probe response p_i is obtained for the probe positioned above A_i, *i.e.*

$$p_i = \sum_{j=1}^{25} \Lambda_{ij}\sigma_j \tag{10}$$

The *global* probe response can then be developed by positioning the probe above each block in turn, *i.e.* for $i = 1 \ldots 25$: see Section 6.

With the probe placed above block 1 ($i = 1$, $x = -10$ mm, $y = 10$ mm), the Λ_1 array is, on the basis of λ_1 and elements Λ_{1j} (9), given in units of 25×10^{-4} mm^2 by

$$\Lambda_1 = \begin{pmatrix} 4161.0 & 936.2 & 196.1 & 76.8 & 34.2 \\ 936.2 & 402.8 & 154.7 & 66.9 & 31.2 \\ 196.1 & 154.7 & 89.3 & 46.5 & 24.1 \\ 76.8 & 66.9 & 46.5 & 28.5 & 16.6 \\ 34.2 & 31.2 & 24.1 & 16.6 & 10.8 \end{pmatrix} \tag{11}$$

This array can also be represented as a 1×25 row matrix, and as such is a sub-matrix of the Λ matrix.

The σ_F array in (5) may be expressed as a 25×1 column matrix. Thus (10) can also be expressed in the form

$$\mathbf{p_i} = \mathbf{\Lambda_i \sigma_F} \tag{12}$$

Upon performing the matrix multiplication of the RHS using the elements of (5) and (11), we obtain (in pC)

$$p_1 = 266.4 \tag{13}$$

Repeating the calculation using the σ_D values, see (7), gives (in pC)

$$p_1 = 228.1 \tag{14}$$

while according to the p array of Yashima *et al.* see (6), their probe response value was measured at (in pC)

$$p_1 = 252 \tag{15}$$

For the probe placed centrally above block 13 ($i = 13$, $x = 0$, $y = 0$), the Λ_{13} array is calculated (units of 25×10^{-4} mm^2) via the λ function to be

$$\Lambda_{13} = \begin{pmatrix} 89.3 & 154.7 & 196.1 & 154.7 & 89.3 \\ 154.7 & 402.8 & 936.2 & 402.8 & 154.7 \\ 196.1 & 936.2 & 4161.0 & 936.2 & 196.1 \\ 154.7 & 402.8 & 936.2 & 402.8 & 154.7 \\ 89.3 & 154.7 & 196.1 & 154.7 & 89.3 \end{pmatrix} \quad (16)$$

From (12) by combining the elements of Λ_{13} and σ_F, we obtain (in pC)

$$p_{13} = 315.4 \quad (17)$$

while upon employing the σ_D values, see (7), gives (in pC)

$$p_{13} = 318.8 \quad (18)$$

Again from the p array, see (6), the measured probe response value was (in pC)

$$p_{13} = 329 \quad (19)$$

Instead of deriving directly the *total* probe response with the probe placed above block 13, the intermediate result before summation can be studied. This gives a clearer picture of how the probe response is made up of the contributions from the surface charges located on the individual blocks. This generates the following array

$$p_{13} = \begin{pmatrix} 3.3 & 5.0 & 6.6 & 0.4 & 2.8 \\ 5.1 & 11.7 & 28.6 & 1.5 & 5.0 \\ 7.0 & 28.6 & 131.1 & 3.3 & 5.9 \\ 2.6 & 11.5 & 32.8 & 1.4 & 4.6 \\ 1.1 & 4.8 & 6.7 & 0.9 & 3.1 \end{pmatrix} \quad (20)$$

or as a total charge (pC), see (17),

$$p_{13} = \sum_{j=1}^{25} p_{13,j} = 315.4 \quad (21)$$

From (20) it can be seen that when the probe is placed above the center of the specimen, only 42% of the total probe response is derived from the block directly beneath the probe (A13), whereas 21% derives from the outer border of blocks. This tendency is still more marked if the composition of the probe response is studied with the probe above block number 14 where the known surface charge has a mimimum value, see (5). In a manner identical to the above, but by using Λ_{14} and σ_F, we evaluate p_{14} to be

$$p_{14} = \begin{pmatrix} 1.7 & 2.9 & 5.2 & 0.5 & 4.9 \\ 2.2 & 4.5 & 12.3 & 3.5 & 13.1 \\ 2.7 & 6.0 & 29.5 & 14.6 & 28.1 \\ 1.1 & 4.4 & 14.1 & 3.3 & 12.1 \\ 0.6 & 2.8 & 5.3 & 1.1 & 5.4 \end{pmatrix} \quad (22)$$

which if expressed as a sum gives

$$p_{14} = \sum_{j=1}^{25} p_{14,j} = 181.9 \quad (23)$$

In this case, the induced charge on the probe deriving from the block directly beneath the probe (A14) amounts to only 8% of the total response. Moreover, although the *actual* charge densities on A13, A14 and A15 are in the ratio of approximately 10:1:10, see (5), the individual contributions from A13 and A15 are remarkedly only twice that of A14 alone. Hence, the contribution from the blocks which do not abutt A14 amounts to as much as 30%, and thus it becomes evident that, when the total response is considered, areas of charge remote from the probe position can play a very significant role.

To derive the global charge distribution, that is to solve for all σ_j using the different p_i, the $25\Lambda_i$ sub-matrices are combined into a 25×25 Λ matrix. Thereafter on the basis of (12) we have

$$\mathbf{p} = \mathbf{\Lambda\sigma} \quad (24)$$

where $\boldsymbol{p}$ is a 25×1 column matrix, in which each element denotes the measured total induced charge on the probe sensor plate for each position of the probe. $\boldsymbol{\sigma}$ is also a 25×1 column matrix with each element representing the surface charge density on the upper surface of one of the blocks. For a given Λ matrix and a measured set of probe responses, (24) can be solved for the unknown σ_j by inverting the Λ matrix: *i.e.* (24) may be re-written as

$$\boldsymbol{\sigma} = \mathbf{\Lambda}^{-1}\mathbf{p} \quad (25)$$

The number of surface elements and that of probe measurements must agree. However, any other division of the surface area may be undertaken, but in each case the surface elements and the set of probe responses must still agree in number. Furthermore, such situations also require that the relevant λ functions be employed. The reason for this rigidity is that, for a given set of probe responses, (25) has one and only one solution.

6. RESULTS: GLOBAL EVALUATTON

Using the probe Λ matrix and the measured probe response, the surface charge densities of the blocks were calculated from (25) using APL software. The results obtained were

$$\sigma_\lambda = \begin{pmatrix} 13.3 & 13.5 & 13.8 & 0.6 & 11.7 \\ 12.9 & 13.2 & 12.3 & 1.4 & 13.3 \\ 14.8 & 13.8 & 13.6 & 1.0 & 12.9 \\ 9.0 & 11.9 & 13.5 & 0.1 & 12.3 \\ 3.8 & 12.9 & 13.3 & 1.3 & 12.9 \end{pmatrix} \quad (26)$$

in μC/m^2, where the subscript λ denotes that the σ values were determined using the λ function. The σ_j elements of σ_λ can be compared with the following σ arrays determined by Yashima *et al.* [4].

As derived from Faraday cage measurements σ_F, see also (5),

$$\sigma_F = \begin{pmatrix} 15.0 & 12.9 & 13.4 & 0.96 & 12.6 \\ 13.3 & 11.6 & 12.2 & 1.5 & 13.0 \\ 14.3 & 12.2 & 12.6 & 1.4 & 12.0 \\ 6.6 & 11.4 & 14.0 & 1.4 & 12.0 \\ 5.0 & 12.4 & 13.6 & 2.3 & 14.0 \end{pmatrix} \quad (27)$$

in μC/m^2.

As calculated from the probe response σ_D, see also (7),

$$\sigma_D = \begin{pmatrix} 11.5 & 12.6 & 11.9 & 1.8 & 9.6 \\ 12.2 & 13.5 & 12.0 & 2.8 & 11.6 \\ 13.3 & 13.9 & 12.8 & 2.5 & 11.3 \\ 8.6 & 12.2 & 12.7 & 1.8 & 10.9 \\ 3.8 & 11.5 & 11.7 & 2.3 & 10.5 \end{pmatrix} \quad (28)$$

in $\mu C/m^2$.

Further, as a means of control on the calculation, the average surface charge density $\bar{\sigma}$ ($\mu C/m^2$) for the 25×25 mm^2 dielectric surface is compared in all three cases:

$$\text{using} \begin{cases} \sigma_\lambda : & \bar{\sigma} = 10.1 \\ \sigma_F : & \bar{\sigma} = 10.1 \\ \sigma_D : & \bar{\sigma} = 9.6 \end{cases} \quad (29)$$

It can be seen that there is excellent agreement between the global charge distribution calculated via the λ function, and that measured by Yashima *et al.* [4] by means of a Faraday cage apparatus. Thus the 2D λ function approach has not influenced adversely the final result.

7. DISCUSSION

7.1. THE PRESENT EVALUATION

As the λ function is simply the proportionality factor between the source charge and the resulting induced charge, the application of this function to the analysis of probe measurements is relatively straightforward. As the λ function is a solution of Laplace's equation, the variation of this function is dependent on the *complete* system geometry. Consequently, for each measuring location of the probe there is a unique λ function, unless a high degree of symmetry exists.

A necessary step in developing a solution for the unknown surface charge density is the discretization of the surface area under study. In this process each of the surface elements is assumed to be a uniformly charged area. With such an assumption, it becomes possible to reduce the basic induced-charge integral, (8), to one involving only the λ function. Due to the discrete nature of the measurement procedure together with the discretization of the surface area, such integrals form the elements of the Λ matrix. This matrix may be referred to as the geometric matrix because it depends only on the geometry of the system and surface elements. Taken together with that of the probe responses, the Λ matrix enables the solution for the unknown surface charge to be obtained. From the present simple geometry, it is clear that any symmetry of the system geometry can be exploited to reduce the amount of numerical calculation associated with the determination of the Λ matrix.

In developing the present analysis, the σ_j results of Yashima *et al.* and the elements Λ_{ij} of the Λ matrix were combined to illustrate how each surface charge element contributed to the total probe response p_i. In this way the individual induced charge contributions could be identified. It is clearly demonstrated that it is possible for areas of charge not situated directly beneath the probe to contribute a significant percentage of the probe signal. Normally, such an analysis can only be undertaken after the global evaluation of σ_j through (25) has been performed. However, in this theoretical exposition σ_j values were available at the onset of the analysis.

In Figure 3, we illustrate the three sets of surface charge densities block by block. It is seen that there is a good agreement among the three different methods. This agreement may be taken as confirmation that the basic assumption in the experimental measurements reported in [4] is, in general, fulfilled; *viz.* that the surface charge was uniformly deposited over the upper surface of each block. A possible exception to this condition may be the blocks of the 4th column on which, although σ was set to zero [4], a finite charge was recorded with the Faraday cage measurements.

In general to solve the basic integral Equation (2), for the unknown surface charge distribution, it is necessary to discretize both the charged surface area and the probe scanning technique. However, the λ function is independent of this process: *i.e.* λ is a continuous function. Hence on the basis of (2), it is possible to examine the response of any probe for a known surface charge distribution. By this means, the characteristics of different probe designs can be examined and evaluated.

7.1.1. LIMITATION OF λ FUNCTION EVALUATION

As mentioned, the evaluation of the λ function was undertaken with a 2 D field program. This implies that, as the calculations were not made on the exact 3D geometry of [4], but on an axially symmetric geometry, then the Λ matrix employed does not comply with the exact boundary conditions in [4]. This approach, however, did provide a simplification in that only one λ function was required in order to generate the Λ matrix. In contrast at least 6 different λ functions would be necessary in the 3D case in order to establish a correct Λ matrix. Although this would require an increase in the data storage, together with a modification to the APL program, the theoretical analysis presented here would remain unaltered.

In an attempt to quantify the degree of approximation introduced by using one axially symmetric λ function, additional calculations were undertaken. For these, a right cylinder of 5 mm diameter was used to simulate a single 5×5 mm^2 block. This representation allows the effect on the λ function approximation to be assessed for probe positions near the edge of the 25×25 mm^2 dielectric block. In comparison with the λ values associated with the 100 mm radius cylindrical block, those for the 2.5 mm radius cylinder are higher along the upper surface: *e.g.* the presence of an edge at $r = 2.5$ mm leads to a 22% increase in the latter λ value at this radial distance. However, with respect to the associated λ-integral, see *e.g.* (9), this deviation reduces to 12%: *i.e.* an integral of this nature is less sensitive to changes in the λ function. As the 2.5 mm radius cylinder is a worst-case situation, the edge error introduced by the lack of 3D software cannot possibly exceed 12%. Consequently, the agreement among the results shown in Figure 3 is maintained.

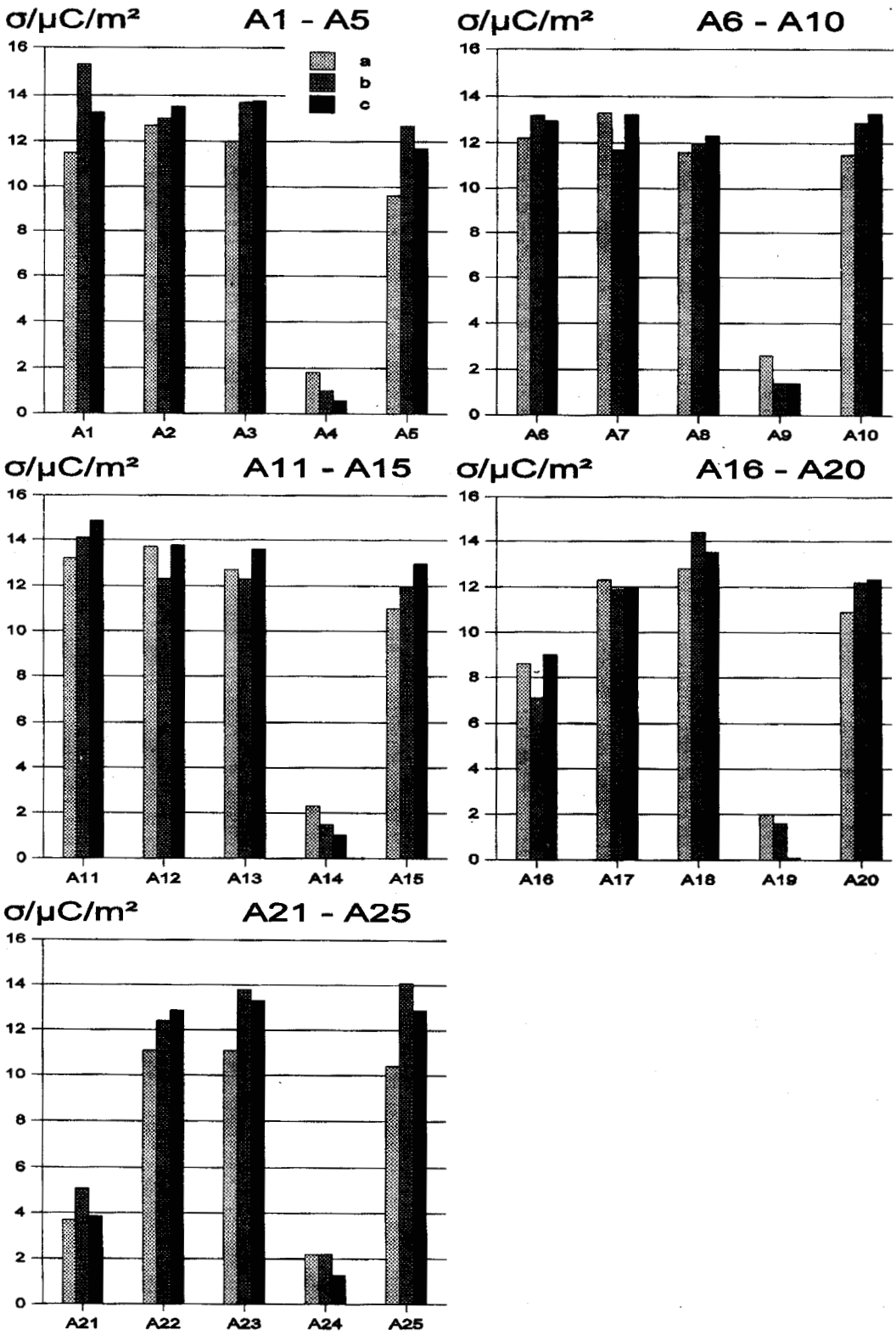

Figure 3. Surface charge density σ on the 25 blocks. (a) multi-point measurement, σ_D [4], (b) measured with a Faraday cage, σ_F [4], (c) determined with the use of the λ function, σ_λ.

7.2. THE EVALUATION BY YASHIMA, FUJINAMI AND TAKUMA

In [4], the matrix equation solved by Yashima and colleagues is expressed as

$$\mathbf{p} = \mathbf{P}_\sigma \tag{30}$$

The $\boldsymbol{p}$ and $\boldsymbol{\sigma}$ matrices are identical with those of the present analysis. Each element of the $\mathbf{P}$ matrix consists of the coefficient P_{ij} which is the response at position i due to a unit charge density at

element j. This coefficient is dependent on the complete system geometry and is determined by a numerical field calculation with the probe sensor plate at zero potential, see Figure 6 of [4]. In this way the Laplacian induced charge is automatically set to zero, so that the Poissonian induced charge can be evaluated directly from the field solution. Each coefficient P_{ij} is then the ratio of the induced charge to the source charge.

If the dielectric surface is discretized into n small surface elements, then P_{ij} will need to be evaluated n times for each of the n positions of the probe. With the λ function approach, λ_i would be evaluated *once* for each of the n probe positions and thereafter Λ_{ij} determined for each of the n surface elements. Thus, although the procedures for determining the P and Λ matrices differ, the two matrices would be identical and hence the two approaches for evaluating the surface charge density are equivalent.

In a separate experiment with a different dielectric geometry, Yashima *et al.* [4] established the importance of charged areas not positioned directly beneath the sensor plate in contributing to the probe response. In the present study, this aspect has been brought fully into focus in a quantitative manner by utilizing the elements of the Λ matrix. The weakness of the circuit-theory approach is now fully in evidence.

7.3. THE EVALUATION BY OOTERA AND NAKANISHI

With all conductors except the sensor plate at zero potential, an expression similar to (24) is also employed in the work of Ootera and Nakanishi [2]. However, their method of deriving the elements of the equivalent Λ matrix is more involved. This situation arises due to the procedure adopted to obtain the electrostatic field solution. In [2], on the assumption that there is no charge within the volume of the dielectric, the dielectric body is represented by a fictitious surface charge density in vacuum. Thereafter the sum of this fictitious charge and the real surface charge is referred to as the apparent charge density. Subsequently these authors use a surface charge method to develop the electrostatic field solution, which is then manipulated to separate the two components of the apparent charge. This process leads eventually to a matrix equation. However, through this approach, each element of the geometical matrix necessarily consists of the product of two sub-elements. Thus the evaluation of this matrix is considerably more complicated than the corresponding Λ matrix. Due to the underlying complexity of the method adopted in [2], the *individual* contributions of the charged surface elements to the probe response are not readily identifiable.

7.4. THE EVALUATION BY SUDHAKAR AND SRIVASTAVA

These authors [5] adopted a surface charge simulation technique [8] to evaluate the surface charge distribution on a spacer. Consequently, the matrix equations which result from the electrostatic field analysis exhibit the same degree of complexity as those obtained by Ootera and Nakanishi [2].

8. CONCLUSION

THROUGH the use of independent experimental measurements, we have demonstrated in detail the λ function approach to the evaluation of electrostatic probe measurements. In this approach, the λ function serves as the link between the data measured with an electrostatic probe and the actual surface charge distribution. Although this function is dependent on the position of the measuring probe in the overall geometry, it is however independent of the discretization of the charged surface area. This feature simplifies the evaluation of the geometric matrix, the Λ matrix, associated with the surface elements. It is through this matrix together with the matrix of the measured probe responses that the unknown surface charge density is determined.

To understand fully the nature of the response of an electrostatic probe it is necessary to examine the intermediate steps in the surface charge evaluation. Such an examination has been undertaken via the λ function, and the significance of contributions to the probe signal from areas of surface charge not directly under the probe have been clearly highlighted. This latter aspect cannot be accounted for when a circuit-theory approach is employed. Thus severe errors in the evaluation of global distributions of surface charge would undoubtedly arise with such an analysis.

In conclusion, only field theoretical solutions can provide a valid evaluation of surface charges on dielectric bodies. The λ function approach provides an elegant solution with added insight.

ACKNOWLEDGMENT

The authors wish to express their gratitude to Dr. M. Yashima and his colleagues of CRIEPI, Tokyo for supplying the numerical data on which Figure 8 of [4] is based.

One of the authors (TOR) wishes to thank the Danish Technical Research Council (STVF) for their considerable financial support during the period of this project.

REFERENCES

[1] D. K. Davies, "The Examination of the Electrical Properties of Insulators by Surface Charge Measurement", J. Sci. Instrum., Vol. 44, pp. 521–524, 1967.

[2] H. Ootera and K. Nakanishi, "Analytical Method for Evaluating Surface Charge Distribution on a Dielectric from Capacitive Probe Measurement - Application to a Cone-type Spacer in ±500 kV DC-GIS", IEEE Trans. Power Delivery, Vol. 3, pp. 165–172, 1988. (presented at the IEEE-PES Summer Meeting, Mexico City, 1986)

[3] A. Pedersen, "On the Electrostatics of Probe Measurements of Surface Charge Densities", in L. G. Christophorou and D. W. Bouldin, *Gaseous Dielectrics* V, Pergamon Press New York, pp. 235–240, 1987.

[4] M. Yashima, H. Fujinami and T. Takuma, "Measurement of Accumulated Charge on Dielectric Surfaces with an Electrostatic Probe", in L. G. Christophorou and D. W. Bouldin, *Gaseous Dielectrics* V, Pergamon Press New York, pp. 242–247, 1987.

[5] C. E. Sudhakar and K. D. Srivastava, "Electric Field Computation from Probe Measurements of Charge on Spacers Subjected to Impulse Voltages", Fifth International Symposium on High Voltage Engineering, Braunschweig, Germany, paper 33.14, 1987.

[6] A. Pedersen, G. C. Crichton and I. W. McAllister, "Partial Discharge Detection: Theoretical and Practical Aspects", IEE Proc. - Science, Measurement and Technology, Vol. 142, pp. 29–36, 1995.

[7] A. Pedersen, G. C. Crichton and I. W. McAllister, "The Functional Relation between Partial Discharges and Induced Charge", IEEE Trans. Diel. and Elect. Insul., Vol. 2, pp. 535–543, 1995.

[8] S. Sato and W. S. Zaengl, "Effective 3-Dimensional Electric Field Calculation by Surface Charge Simulation Method", IEE Proc. A, Vol. 133, pp. 77–83, 1986.

Manuscript was received on 11 April 1996.